Degradation of aniline in groundwater by persulfate with natural subsurface sediment as the activator

Nasiru Abba Mustapha [a,b], Hui Liu [a,*], Abdullateef Omeiza Ibrahim [a], Yao Huang [a], Shan Liu [a]

[a] State Key Laboratory of Biogeology and Environmental Geology and School of Environmental Studies, China University of Geosciences, Wuhan 430074, PR China
[b] Department of Environmental Sciences, Federal University Dutse, Jigawa State, Nigeria

ARTICLE INFO

ABSTRACT

Aniline is reported as a toxic contaminant in the groundwater at some industrial sites. Persulfate oxidation is a promising method to degrade aniline. However, the lack of appropriate activation method limited its application in extensive engineering of groundwater remediation. This paper aims to evaluate the feasibility of aniline degradation in groundwater by persulfate with *in-situ* subsurface sediment as an activator. Our findings suggested that the Fe(II)-O complex in sediment interacted with persulfate to produce $SO_4^{\cdot-}$, $OH^{\cdot}$ and Fe(IV) as indicated by the radical scavenging studies. Interestingly, data further revealed that the presence of the sediments simultaneously induced a non-radical mechanism in the degradation process that oxidized aniline to form two aminophenol isomers and azoxybenzene (first detected), which possibly mineralized as indicated by the significant amount of TOC removal in 24 h. The stoichiometric efficiency of the treatment system was substantial in all evaluated conditions. It was notably enhanced by increasing either the initial amount of persulfate, aniline or mass of aquifer sediments. These results confirm that the persulfate without other high-cost activation technologies can be used for *in-situ* remediation of aniline contaminated groundwater as the sufficient subsurface sediment is an excellent activator and urge the reassessment when employing this technique for remediation purposes since each contaminant may demonstrate a different degradation mechanism.

1. Introduction

Groundwater serves as the primary source of local drinking water in most rural communities [1]. However, groundwater quality has been progressively deteriorated due to natural and anthropogenic activities [1]. Aniline is a toxic compound that can cause neurological damage, a shutdown of the cardiovascular system, liver and kidney failures [2]. Unfortunately, many reports indicate that significant amounts of aniline have been detected in aquifer systems and groundwater samples at several abandoned industrial sites [3–6]. Consequently, the continuous use of this groundwater resource could induce severe health threats to human beings [7]. Thus, the remediation of aniline contaminated groundwater causes great concern.

In-situ chemical oxidation (ISCO) provides a promising technique for remediating recalcitrant organic contaminants in subsurface environments such as aquifer [8]. Previously, the most common oxidants used for groundwater remediation are peroxymonosulfate, permanganate, ozone, and hydrogen peroxide [9–11]. Recently, many investigations have devoted their attention towards using persulfate as an oxidant for

ISCO due to its wide application range of contaminant degradation at circumneutral pH compared to other commonly used oxidants [12–14]. Persulfate ($E^0 = 2.01$ V) is usually activated to generate powerful sulfate radicals ($SO_4^{\cdot-}$) with a high standard oxidation-reduction potential of 2.6 V, capable of oxidizing and degrading numerous organic contaminants [15,16]. A lot of methods such as heat, ultrasound, transition metal ions, and carbonaceous materials have been used in previous studies to activate persulfate [8,17–19], which indicates a wide range of techniques can enable persulfate oxidation [16]. However, the use of these persulfate activation procedures in the subsurface environment is not feasible due to the difficult engineering challenges and a tremendous amount of logistics involved.

The potential application of activated persulfate in aniline degradation has been explored using different persulfate activation techniques like rice straw biochar [20], zero-valent iron (ZVI) [21], electrochemical activation [22], ultrasound [23], heat activation [24]. However, these technologies are challenging to be used for sizeable *in-situ* remediation engineering due to aquifer blockage, large consumption of energy, and high maintenance cost, etc. Therefore, the development

of feasible persulfate activation methods is demanding for the practical application of persulfate in groundwater remediation.

Subsurface sediment contains a significant amount of iron-bearing minerals that potentially activate persulfate [25,26]. The practicability of aquifer sediments to be used as a possible *in-situ* activator of persulfate has been investigated for the remediation of 1,4-dioxane in groundwater [27]. However, the removal of dioxane was less than 20% after 36-h persulfate oxidation with four types of subsurface media as the activators [27].

Aniline, as an electron-donating compound, showed a high reaction rate with sulfate radical (Eq. (1)) [28].

$$aniline + SO_4^{\cdot -} \rightarrow aniline^{\cdot +} k = 7.7 \pm 0.5 \times 10^9 \ M^{-1} \ s^{-1} \qquad (1)$$
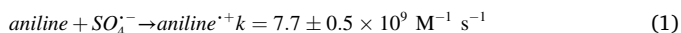
Therefore, it is hypothesized that aniline in groundwater may be efficiently degraded by the injected persulfate activated by the *in-situ* subsurface sediment. On the other hand, groundwater components such as bicarbonate (HCO_3^-), chloride (Cl^-), and natural organic matter (NOM) may influence aniline degradation as they can also consume sulfate radicals [29–31]. One concern is that these groundwater components may serve as radical scavengers and limit the extent of aniline degradation.

This paper aims to evaluate the feasibility of aquifer sediments activation of persulfate for *in-situ* aniline contaminated groundwater remediation. Anaerobic and dark conditions were maintained for all experiments to mimic the conditions of the aquifer. Degradation kinetics of aniline were determined at various levels of persulfate, aquifer sediments, aniline, HCO_3^-, Cl^-, and NOM. Potential mechanisms responsible for free radical production, and pathways for aniline degradation are presented.

2. Materials and methods

2.1. Site description and sediment sampling

Aquifer sediment samples were collected from Zhongxiang city (31.042484°N, 112.653342°E), Hubei province, China. Descriptive regional hydrogeology and sediment profile are provided formerly [32]. The groundwater level is approximately 3 m at the site. Therefore, the aquifer sediments at a depth of 4–5 m was collected. A hand-held soil-sampling rig (Chrisite SD-1, Beijing, China) equipped with 1 m PVC pipes were used to collect aquifer sediment samples. Each 1 m PVC pipe was divided into five segments. The end of each section was immediately sealed with a sealing cover, and each part was wholly wrapped with aluminium foil paper and stored in a plastic vacuum bag to preserve the anaerobic condition of aquifer sediment and avoid exposure to light. The aquifer sediment samples were transported to the laboratory and preserved based on procedures used in a previous study [33].

2.2. Chemicals

Aniline (C_6H_7N), sodium persulfate ($Na_2S_2O_8$), ferrous sulfate heptahydrate ($FeSO_4 \cdot 7H_2O$), sodium bicarbonate ($NaHCO_3$), potassium iodide (KI), and sodium chloride (NaCl) were all purchased from Sinopharm Chemical Reagent Co., Ltd (Shanghai, China). Methyl phenyl sulfoxide (PMSO) (98%) and humic acid (HA) was obtained from Shanghai Macklin Biochemical Co., Ltd (Shanghai, China). HA was used as a representative of NOM [34].

2.3. Batch experimental procedures

All experiments were carried out in an anaerobic glove box (Mikrouna Co., Ltd., Beijing, China) filled with Ar (99.99%) to keep O_2-free conditions. Deionized water was purged with N_2 gas to remove O_2 before the commencement of each experiment. Fresh stock solutions of aniline and persulfate were also prepared in the N_2-purged deionized

water before the start of each operation. For aniline degradation experiments, the aquifer sediment was mixed with aniline solution first. The degradation experiments were commenced by the addition of stock persulfate solution in a glass bottle in the anaerobic glove box. Two control experiments were included: one consisting of aniline with aquifer sediments but without persulfate, while the other contained aniline and persulfate but no sediment. The pH values in all experiments were from 6.8 to 7.8 and without further adjustment. The sealed reactors were kept in the dark by being wrapped with foil paper. Then, the reactors were taken out of the glove box and placed on a rotary shaker (150 rpm, 25 ± 1 °C). All the reactions were operated as entirely mixed batch reactor systems. At predetermined intervals, aliquots of 0.5 mL samples were taken from each sealed reactor using a sterilized syringe, then filtered through a 0.22-μm nylon filter, and the oxidation reaction was immediately quenched utilizing an ice bath based on previous protocols [22]. The collected samples were immediately subjected to component analysis. All experiments were performed in duplicates, and average results are reported.

Other experiments were conducted as above to investigate the influences of the initial levels of aniline (0.05–1 mM), persulfate (0–50 mM), sediment (0–30 g in 50 mL reaction system), HCO_3^- (0–100 mM), Cl^- (0–100 mM), and HA (0–100 mg C L^{-1}). Besides, different quenching experiments were conducted to explore the possible generation of $SO_4^{\cdot -}$, $OH^\cdot$ and other active species such as Fe(IV). Details of the procedures are described as Text S1 in the Supporting material section

2.4. Analysis and characterization procedures

The concentration of aniline in the aqueous phase was measured by the high-performance liquid chromatography (HPLC) (LC-20AD, Shimadzu Co., Japan) equipped with a UV detector set at 230 nm and Kromasil C18 column (150 mm × 4.6 mm, internal diameter 5 μm, Amsterdam, Netherland). The mobile phase consisted of acetonitrile and ultra-pure water (65:35, v/v) at a flow rate of 0.5 mL min^{-1}. The column temperature was set at 40 °C, and the injection volume was 20 μL.

The intermediates for aniline degradation were analyzed using high-performance liquid chromatography–high-resolution mass spectrometry (HPLC–HRMS) (Dionex UlitiMate 3000, Dionex, USA). The HPLC system was equipped with a Kromasil C18 column (150 mm × 4.6 mm, i.d. 5 μm, Amsterdam, Netherland). All possible intermediates were eluted orderly from the column in a single chromatography run using a gradient elution program. The mobile phase was ultra-pure water (A) and HPLC grade acetonitrile (B). The gradient was used as follows: 90% B and 10% A held for 8 min at the beginning, and then changed to (80% A and 20% B) for 2 min. There was a one-min equilibration time needed before the next injection. Five microliters of sample were injected using an autosampler. The column oven temperature was kept at 40 °C, and the flow rate was set at 0.2 mL min^{-1}. Identification of aniline degradation intermediates was conducted using a Q Exactive mass spectrometer (Thermo Fisher Scientific, USA) in positive ion spectra under electrospray ionization (ESI+) source. The data were analyzed using the software Xcalibur 2.1 (Thermo Fisher Scientific, USA) based on a method described in our previous study [35].

Persulfate decomposition was measured by a spectrophotometric method with potassium iodide and sodium bicarbonate at 352 nm [36]. Total organic carbon (TOC) in the aqueous solution was quantified using a non-purgeable organic carbon (NPOC) method on a Shimadzu TOC-L analyzer (Shimadzu, Japan). At the same time, the TOC of the aquifer sediment was measured on a carbon-sulfur analyzer (Jena multi-EA 4000, Germany). X-ray photoelectron spectroscopy (XPS) (PHI 5000 VersaProbe, U1VAC-PHI, Japan) was performed to examine the changes of Fe species after the experiments. The XPS employed a monochromated A1Ka X-ray source. The binding energy of the C(1s) level at 284.6 eV was taken as an internal reference to calibrate energy spectrum. High-resolution spectra of Fe2p3/2 were collected and fitted using a least-square procedure with Gaussian-Lorentzian peak shapes in

Xpspeak41 software after subtracting the baseline. The BET surface area was determined according to the multipoint N_2 adsorption-desorption method using a Surface Area & Pore Size Analyzer (Micromeritics ASAP 2460, USA). The metal concentrations of subsurface sediment were analyzed with an inductively coupled plasma optical emission spectrometer (ICP-OES, Agilent, 720) while the contents of SO_4^{2-} and Cl^- were detected using an ion chromatograph (Dionex 2500, USA). The mineral composition was analyzed using a D/MAX-RB powder X-ray diffractometer (Rigaku Corporation, Japan) at room temperature. Cu Kα radiation (λ = 0.15418 nm), with a step size of 0.02° in the 2θ range from 5° to 65°. The data were analyzed with XrayRun 2.0 software, and the peaks were identified according to a recent study [37]. Contents of Fe(II), Fe(III), and total Fe in the solid phase of the sediment were analyzed according to the literature [33]. Briefly, a specified amount of the aquifer sediments was digested by HF and H_2SO_4 at 100 °C. The dissolved Fe(II) solutions were determined at 510 nm using 1,10-phenanthroline method. Total Fe was analyzed by reduction of Fe(III) by addition of 10% hydroxylamine hydrochloride [33]. The main physicochemical properties of the subsurface sediment are displayed in Table 1.

3. Results

3.1. Persulfate decomposition and stoichiometry efficiency

Persulfate decomposition in different conditions are presented in Fig. 1. The concentration of persulfate remained approximately the same during the experiment without the addition of sediments nor aniline. No loss of persulfate was also observed in the control experiments consisting of only aniline and persulfate. A negligible amount of persulfate decomposed in the presence of only the aquifer sediments under the experimental conditions. However, Fig. 1 shows that the concentration of persulfate decreased in the experiments consisting of the aquifer sediments and aniline. Persulfate decomposition was slightly enhanced in the presence of HCO_3^- (0–50 mM), Cl^- (0–100 mM) and NOM ((0–100 mM) with the exception of higher amounts of HCO_3^- (100 mM) (Table S1), while increasing the concentration of aniline (0–1 mM) accelerated the decomposition rate of persulfate (Fig. S1). The data (Table S1) further revealed that increasing the initial amount of persulfate (5–50 mM) considerably decreased persulfate decomposition.

The stoichiometry between the amount of aniline (moles) degraded for every mole of persulfate decomposed was determined based on protocols employed in previous studies [38,39]. Depending on the treatment condition (Table S1), the result revealed that the stoichiometric efficiency of the degradation process was significant and varied considerably, from 2.53 to 51.66%. The highest stoichiometric efficiency achieved was when persulfate concentration was at 50 mM. However, Fig. S2 also revealed that increasing the mass of sediment (0–30 g) and aniline concentration (0 – 1 mM) had a positively linear correlation with stoichiometric efficiency.

Table 1
Physicochemical properties of the subsurface sediment.

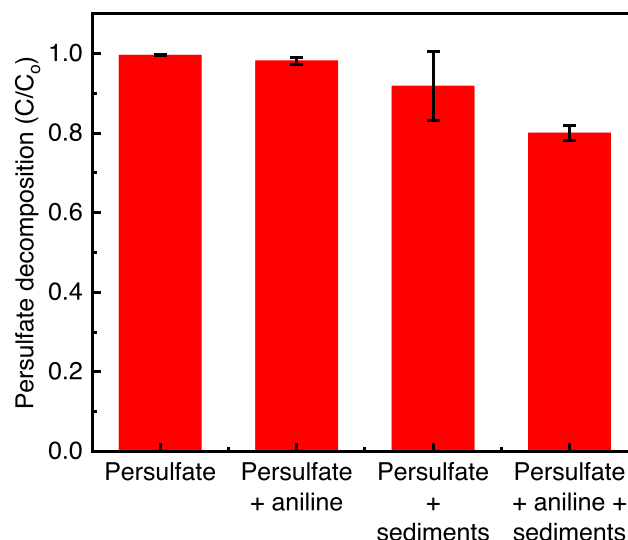| Parameters	Contents	Parameters	Contents
Fe*	35.36	Cu*	0.07
Fe(II)*	17.46	Zn*	0.34
Fe(III)*	17.90	Cr*	0.04
Mg*	20.61	SO_4^{2-} (mg kg^{-1})	525.4
Al*	33.40	Cl^- (mg kg^{-1})	108.3
Ca*	44.11	TOC*	4.85
K*	6.42	BET (m^2 g^{-1})	5.65
Na*	0.70	pH	7.99
Mn*	not detected	Texture	Fine sand

*Contents in mg g^{-1}.

Fig. 1. Persulfate decomposition in different conditions including persulfate alone, and in the presence and absence of aquifer sediments and aniline. [PS]$_o$ = 10 mM, sediment mass = 10 g, [AN]$_o$ = 0.5 mM, T = 25 ± 2 °C, Volume = 50 mL. Experiment duration = 6 h.

3.2. Aniline degradation kinetics under various conditions

The kinetics of aniline degradation by persulfate and subsurface sediment under different conditions are shown in Fig. 2. The aniline concentrations showed no significant change in the reactor without persulfate (Fig. 2a), indicating that neither evaporation nor adsorption of aniline on the sediment occurs. Besides, in the reactor without sediment (Fig. 2b), aniline did not decline, too, suggesting that persulfate is unable to degrade aniline directly in our system. However, the mixture of persulfate with sediment caused a significant decrease in aniline concentration in 6 h under the experimental conditions. The higher level of persulfate and the lower dose of aniline caused a more rapid reduction of aniline (Fig. 2a and c). The increase of sediment amount from 10 to 30 g induced a slightly faster decline of aniline (Fig. 2b). In 6 h, more than 90% aniline was removed when the persulfate concentrations varied from 10 to 50 mM, the sediment amounts from 10 to 30 g, and the aniline concentrations from 0.05 to 1.0 mM in 50 mL reaction system. Only 77% of aniline was degraded when the persulfate concentration was as low as 5 mM. To quantitatively compare the aniline degradation kinetics under different conditions, a pseudo-first-order kinetic model was used to fit the dynamic data, and the rate constant of aniline degradation was computed as below.

$$lnC_t = lnC_o - kt \qquad (2)$$

where C_o is the initial concentration of aniline (mM), C_t is the concentration of aniline at the designated time (mM), k is the rate constant of aniline degradation (h^{-1}), and t is time (h). The r^2 for the simulation of results under all conditions were from 0.867 to 0.999.

The relationships between k values and the levels of persulfate, sediment, and aniline were illustrated in Fig. 3. The rate constant of aniline showed a positively linear correlation with persulfate concentration from 0 to 50 mM (Fig. 3), following the equation $y = 0.039x + 0.002$, $r^2 = 0.998$. The increase of sediment amount from 0 to 10 g in 50 mL reaction system caused a fast rise in the rate constant and then slowed down with the further increase of sediment amount from 10 to 30 g. However, no inhibition was observed in the amount of aniline removed. The relationship between sediment amount and rate constant fits the exponential model $y = 6.774 - 0.675 \exp(-0.165 x)$, $r^2 = 0.999$. The rate constant decreased with the increasing of aniline concentration from 0 to 1.0 mM, and their relationship was well consistent with the
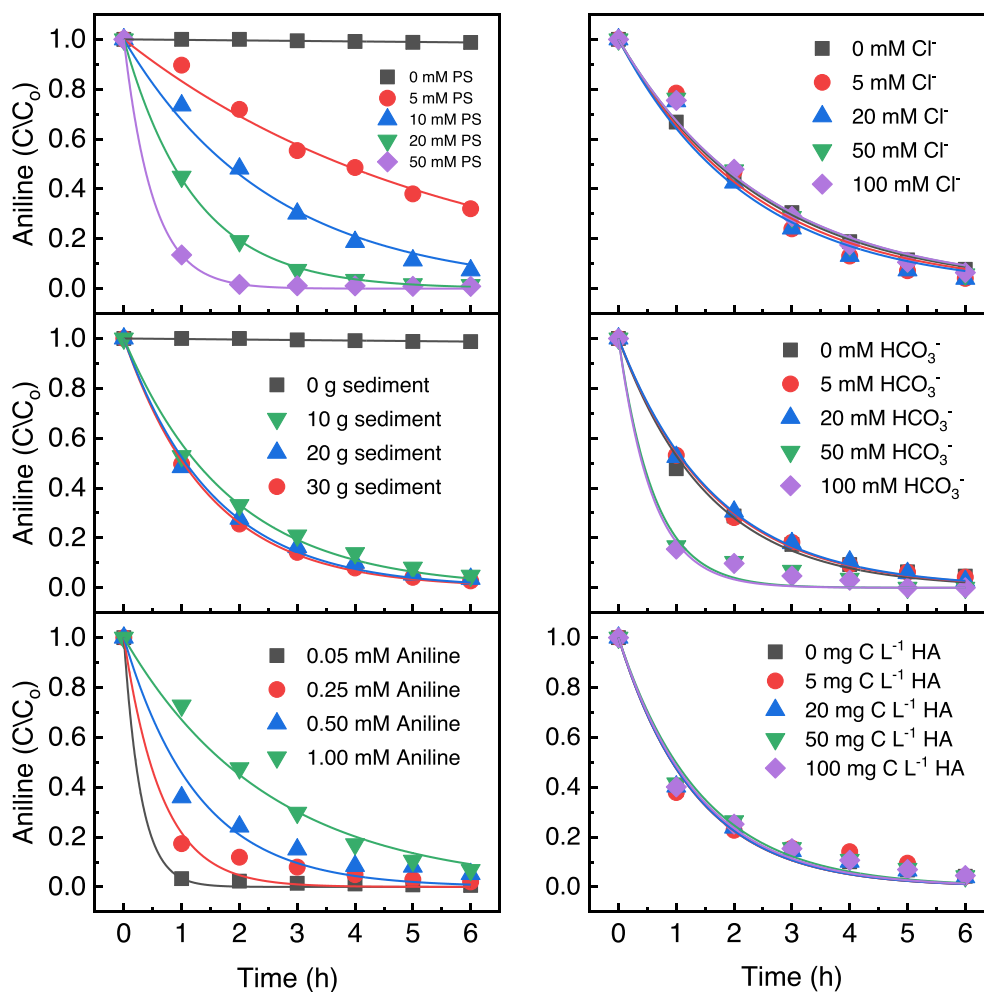
Fig. 2. Aniline degradation kinetics with pseudo-first-order model fittings (solid curves) at (a) different concentrations of persulfate 0.0–50 mM, sediment mass = 10 g, $[AN]_o$ = 0.5 mM, T = 25 ± 2 °C, Volume = 50 mL; (b) different levels of sediment mass 0–30 g, $[PS]_o$ = 10 mM, $[AN]_o$ = 0.5 mM, T = 25 ± 2 °C, Volume = 50 mL; (c) different initial concentrations of aniline 0.05–1.00 mM, $[PS]_o$ = 10 mM, sediment mass = 10 g, T = 25 ± 2 °C, Volume = 50 mL; (d) different concentrations of Cl^- 0.0–100 mM, $[PS]_o$ = 10 mM, sediment mass = 10 g, $[AN]_o$ = 0.5 mM, T = 25 ± 2 °C, Volume = 50 mL; (e) different concentrations of HCO_3^- 0.0–100 mM, $[PS]_o$ = 10 mM, sediment mass = 10 g, $[AN]_o$ = 0.5 mM, $[HCO^-_3]$ = T = 25 ± 2 °C, Volume = 50 mL; (f) different concentrations of humic acid (HA) 0.0–100 mM, $[PS]_o$ = 10 mM, sediment mass = 10 g, $[AN]_o$ = 0.5 mM, $[HA]$ = T = 25 ± 2 °C, Volume = 50 mL.

exponential model $y = 0.353 + 3.690 \exp(-4.371 x)$, r^2 = 0.997. The levels of Cl^- (0–100 mM), HCO_3^- (0–20 mM), and HA (0–5 mg C L^{-1}) induced no significant deviation of aniline removal (Fig. 2d–f). The higher concentrations of HCO_3^- (50 and 100 mM) caused faster aniline degradation. The rate constants of aniline degradation in the presence of 50 and 100 mM were 1.607 ± 0.19 and 1.695 ± 0.18 h^{-1}, respectively, whereas those in the presence of 0–20 mM were from 0.635 ± 0.03 to 0.596 ± 0.01 h^{-1}.

3.3. Iron species on the sediment before and after the reaction

In the oxidation process, no dissolved Fe was detected in the solution. To determine the Fe species in the solid phase participated in persulfate activation, XPS was employed. The results showed five peaks at 709.5, 710.7, 711.7, 712.6, and 714.0, corresponding to Fe(II)-O complex [40], FeCO$_3$ [40,41], Fe(III)-O/H(1) [42,43], Fe(III)-O/H(2) [44] and Fe(III) sulfate [40], respectively (Fig. 4). Before reaction, Fe(II), as forms of Fe (II)-O complex and FeCO$_3$, occupied 48.1% of total Fe on the surface of the sediment, and Fe(III), as species of Fe (III)-O/H(1), Fe(III)-O/H(2) and Fe(III) sulfate, were 51.9% of total Fe. After the reaction, Fe(II)-O complex decreased from 25.0 to 14.7% and correspondingly Fe(III)-O/ H(1) increased from 18.6 to 24.9%. Other Fe species showed only slight changes.

The aquifer sediments were also characterized by XRD to evaluate the interactions of the Fe species before and after oxidation reactions. The XRD patterns showed that there were noticeable variations in the relative peak intensities of the mineral composition of Fe containing minerals like illite, amphibole and chlorite. As shown in Fig S3, the peak

intensities of chlorite and illite decreased, whereas a noticeable increase of the peak for amphibole was observed after oxidation reactions.

3.4. Identification of dominant free radical species for aniline degradation

The aniline degradation kinetics in the presence of different quenching agents are illustrated in Fig. 5a, and the degradation rates (Fig. 5b) of aniline were also computed according to Eq. (2). Ethanol, methanol and TBA are commonly used as radical scavengers to determine the roles of SO_4^{-} and $OH^{\bullet}$ [45,46]. PMSO was used as a probe compound to explore the possible generation of Fe(IV) species in the reaction system due to its rapid reactivity with Fe(IV) as reported in recent studies [47,48]. The addition of 1 M TBA significantly reduced the degradation rate of aniline from 0.712 ± 0.04 to 0.417 ± 0.03, suggesting that $OH^{\bullet}$ plays a role in aniline degradation. On the other hand, the aniline degradation rate declined to 0.307 ± 0.03 and 0.358 ± 0.01 after addition of 1 M ethanol and methanol respectively, indicating that SO_4^{-} also participated in aniline degradation. The degradation rate also decreased to 0.429 ± 0.01, in the presence of 0.5 mM PMSO, showing the possibility of Fe(IV) participating in the degradation system. The formation of Fe(IV) in the oxidation system was verified by the transformation of PMSO to PMSO$_2$ (Fig. S4) [47]. However, it is noticeable that the aniline degradation had not been wholly stopped despite the individual addition of PMSO, ethanol, methanol and TBA into the reaction system to quench Fe(IV), SO_4^{-} and $OH^{\bullet}$ respectively.
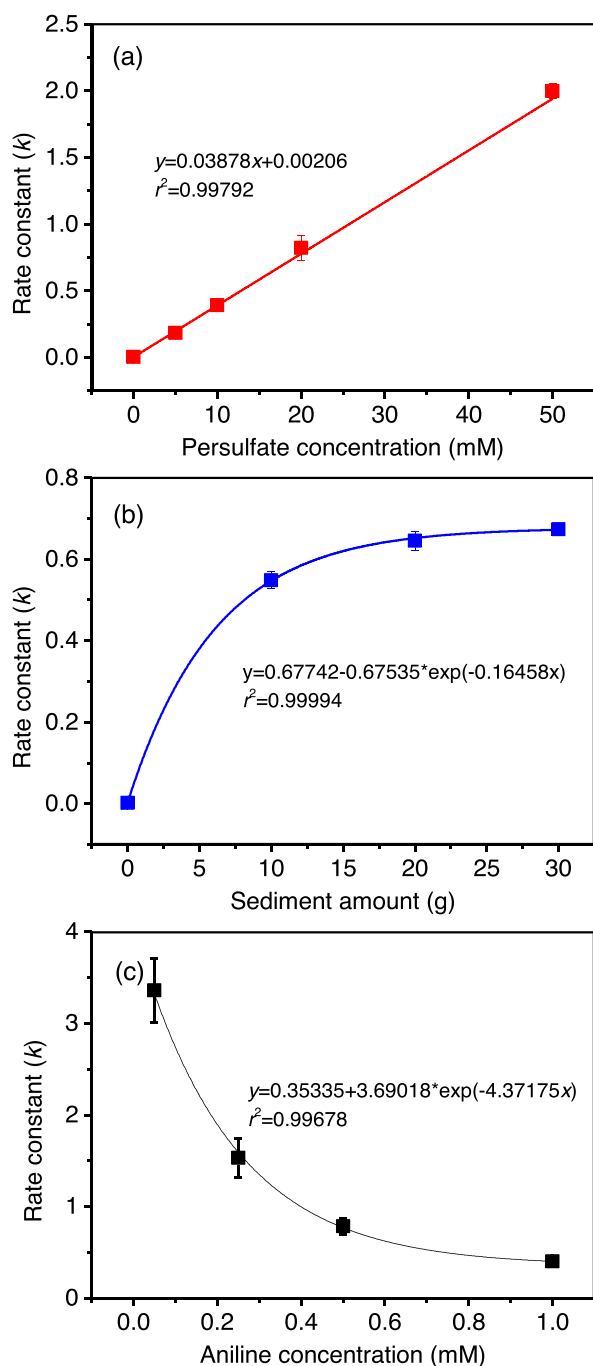
Fig. 3. Correlation between rate constants of aniline degradation and levels of persulfate (a), sediment (b), and aniline (c). The curves are the simulated results.

Fig. 4. XPS spectra of Fe($2p_{3/2}$) for the subsurface sediment (a) before and (b) after 6-h experiment. The experimental conditions: $[AN]_o$ = 0.5 mM, $[PS]_o$ = 10 mM, sediment mass = 10 g, volume = 50 mL, T = 25 ± 2 °C.

Fig. S6. The intermediate at 4.85 min was produced in 2-h reaction sample and kept at a low level afterwards. Meanwhile, the intermediate at 3.35 min was detected in 2 h and declined fast in the next 6 h, and then slowly decreased to zero in the next 16 h. The intermediate at 5.80 min kept increasing in the first 4 h and then gradually reduced to zero in the next 20 h.

According to the retention times in HPLC chromatographs, the computational studies on the Boyland-Sims oxidation [49,50], and the kinetics of intermediates, the two isomers at 3.36 and 4.83 min were proposed to be phenylhydroxylamine and 4-aminophenol, respectively, and the compound at 5.80 min was assigned as azoxybenzene.

4. Discussion

4.1. The efficiency of aniline degradation by sediment-activated persulfate oxidation

Our findings have demonstrated that aniline can be significantly degraded by persulfate in the presence of subsurface sediment. In 6 h, more than 90% aniline was removed when the persulfate concentrations were from 10 to 50 mM, the sediment amounts from 10 to 30 g, and the aniline concentrations from 0.05 to 1.0 mM in 50 mL reaction system. The results also demonstrated that the rate of persulfate consumption in the degradation process decreased in the presence of higher amounts of persulfate and mass of sediments, respectively, while increasing the concentration of aniline accelerated persulfate decomposition. The data similarly revealed that the efficiency of the treatment system was significant in all evaluated conditions. The stoichiometric efficiency was

3.5. Determination of aniline degradation intermediates

The intermediates of aniline degradation were identified on HPLC-HRMS, and the results were analyzed using the software Xcalibur 2.1 [35]. Fig. S5 showed that three intermediates were identified. The same mass ratio (m/z 110.06019) appeared at two different retention times, 3.35 and 4.85 min, respectively, indicating the formation of an isomer. The elemental composition analysis showed that the formula of them was C_6H_7ON with a delta of 1.359 ppm. Another intermediate was detected at 5.80 min with m/z 199.08691. The formula of it was assigned to $C_{12}H_{10}ON_2$ with the delta of 1.610 ppm. The relative dynamics of the intermediates with aniline degradation are shown in
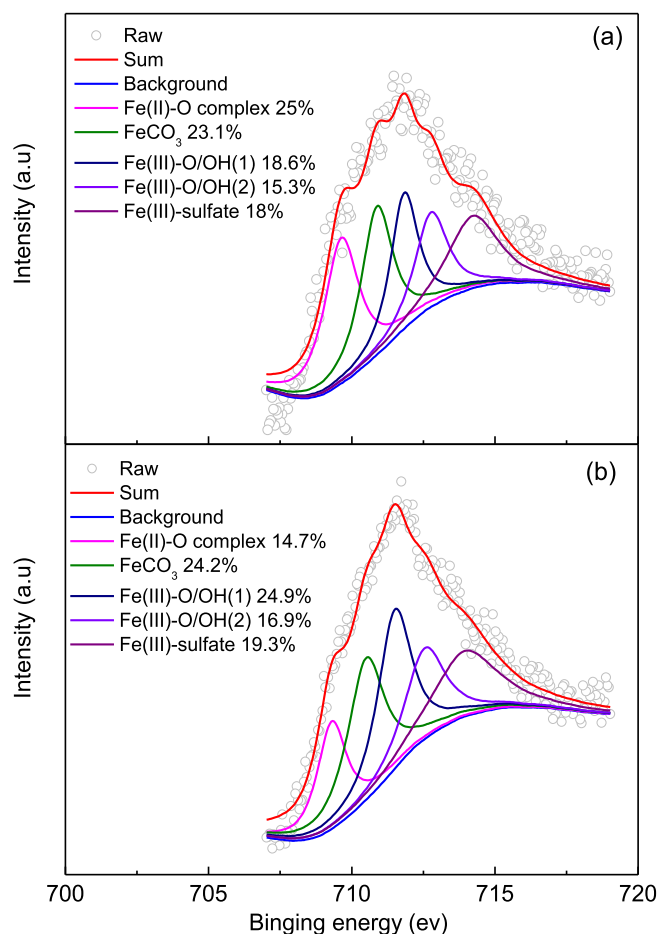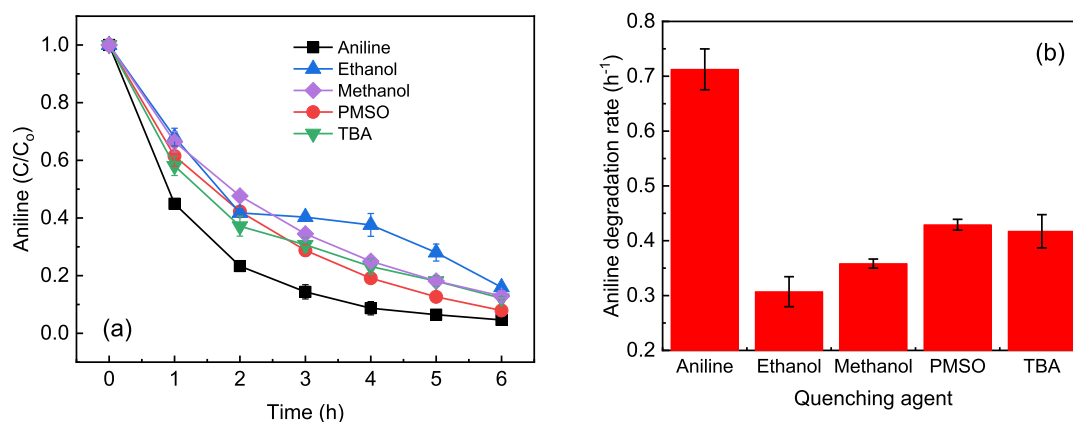
Fig. 5. (a) Effects of radical scavengers ethanol, methanol, methyl phenyl sulfoxide (PMSO) and *tert*-butyl alcohol (TBA) on the degradation of aniline in the sediment–activated persulfate system. (b) Effects of radical scavengers on rate constants of aniline degradation. Experimental conditions: $[AN]_o = 0.5$ mM, $[PS]_o = 10$ mM, [ethanol] = 1 M, [methanol] = 1 M, [PMSO] = 0.5 mM, [TBA] = 1 M, sediment mass = 10 g, T = 25 ± 2 °C, volume = 50 mL.

notably enhanced by increasing the initial amount of persulfate, aniline and mass of aquifer. On the other hand, the effects of groundwater components Cl^-, HCO_3^-, and NOM induced a negligible influence except higher concentrations of HCO_3^- (50–100 mM).

Some studies concerned the attenuation in toxicity with the destruction of degradation byproducts in persulfate oxidation systems [51,52]. Likewise, in the study herein, complete degradation of byproducts was observed as indicated by the relative dynamics of the intermediates with aniline degradation reported in Fig. S6. The considerable amount of TOC removal (53.25% after 24 h) as illustrated in Fig. S7 further supports this observation. It indicates that, in the oxidation reaction process, aniline, together with the identified degradation intermediates, was not only degraded but also mineralized [20,21]. Therefore, these observations suggest that this oxidation system is effective in controlling the toxicity of aniline degradation [51,52].

Compared with the activation methods used before, the aquifer sediment is of relatively high efficiency to activate persulfate for aniline degradation under groundwater conditions. Most related studies (Table S2) reported that increasing the amount of persulfate decreased aniline removal and stoichiometric efficiency, respectively [20,53]. The concentration of persulfate used in field applications (42 mM) is higher than the reported amounts used in these studies [20,53,54], and this might significantly enhance persulfate consumption.

Collectively, our results indicated otherwise. For the *in-situ* remediation of aniline contaminated groundwater, direct injection of persulfate to the aquifer is efficient to degrade aniline due to the activation of persulfate oxidation by the *in-situ* sediment.

4.2. The mechanism on the aniline degradation by sediment-activated persulfate oxidation

Subsurface materials contain a significant amount of iron-bearing minerals that can activate persulfate oxidation [25,33] which has been proven to degrade benzene and 1,4-dioxane in groundwater [26,27]. Sra et al. (2010) reported that the decomposition of persulfate activated by aquifer sediments was highly dependent on the content of sediment-bound active iron and TOC [25]. It is also hypothesized that iron associated with the aquifer sediment is primarily responsible for the activation of persulfate, and the degree of degradation enhancement of 1,4-dioxane relates in part to dissolved-phase iron content [27]. Moreover, Liu et al. demonstrated that Fe(III)- and Mn(IV)-oxides in aquifer sediment catalytically converted persulfate into SO_4^- and OH [26]. These observations are consistent with the findings in our study. The XPS and XRD results demonstrated the surface-catalyzed reactions between persulfate and iron-containing minerals associated with the aquifer sediments [25,26]. As shown in (Fig. 2), the Fe(II)-O complex

in the subsurface sediment was oxidized to Fe(III)-O/H(1) in the process of aniline degradation by persulfate since there was no detectable dissolved Fe in the reaction solution. Some reports suggested that Cu and manganese oxides can also activate persulfate [27,45]. However, the ICP–OES data presented in Table 1 indicated that Fe is several magnitudes higher than Cu while Mn was below detection. The XRD results (Fig. S3) further revealed that the aquifer sediments contain substantial amounts of Fe bearing minerals. It is well established that homogeneous or heterogeneous activation of persulfate by transitional metals like Fe^{2+} is predominantly effective under acidic conditions [16,21,45,53]. However, the significant changes observed in the Fe(II)-O complex and corresponding Fe(III)-O/H(1) in addition to the increase in the composition of ferrous containing minerals illite and chlorite as shown by the XRD patterns indicated that the contribution of Fe(II)-O complex in the degradation process occurred under circumneutral pH conditions.

Results from quenching studies demonstrate that SO_4^- and OH play essential roles in aniline degradation. Previous research has proposed that the Fe(II) on the aquifer sediment surface can be oxidized rapidly by persulfate to generate Fe(III) with the production of SO_4^- ($E^0 = 2.6$ V) and sulfate [26].

$$\equiv Fe(II) + S_2O_8^{2-} \rightarrow \equiv Fe(III) + SO_4^{2-} + SO_4^{\cdot-} \qquad (3)$$
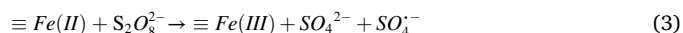
Meanwhile, $SO_4^{\cdot-}$ can produce OH ($E^0 = 2.7$ V) in aqueous solution following the reaction below.

$$SO_4^{\cdot-} + H_2O \rightarrow SO_4^{2-} + OH^{\cdot} + H^+ \qquad (4)$$

Additionally, a recent study (Eq. (5)) demonstrated the generation and participation of Fe(IV) in ferrous iron persulfate activated systems at circumneutral pH [47].
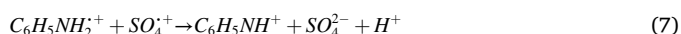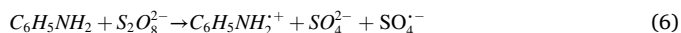
$$Fe^{2+} + S_2O_2^{2-} + H_2O \rightarrow Fe^{IV}O^{2+} + 2SO_4^{2-} + 2H^+ \qquad (5)$$
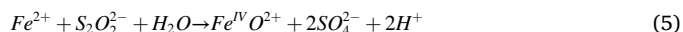
In our experiment systems, there is no dissolved Fe^{2+} detected. However, the formation of $PMSO_2$ confirmed the formation of Fe(IV) (Fig. S5) suggesting that the Fe(II) on the aquifer sediment surface can also activate persulfate to produce Fe(IV). The slight inhibition of the degradation rate of aniline by the addition of PMSO (Fig. 5b) indicated the contribution of Fe(IV) in the degradation process [47]. We should note that aniline is an electron-donating compound. Meanwhile, a recent report has suggested that Fe(IV) selectively reacts with electron-rich organic compounds [55], indicating that aniline will also compete for the available Fe(IV) in the degradation system [55] However, data presented in Fig. S4 revealed that less than 30 μM Fe(IV) was produced. Consistent with the previous related studies [55], Fe(IV) was generated in the reaction system but induced a negligible contribution towards aniline removal in the degradation process.

It was proposed that the degradation of aniline in persulfate-ZVI

system is initiated by the attack of SO_4^{-} and $OH^{\bullet}$ and forms aniline cation radicals ($C_6H_5NH_2^{\bullet+}$), then is oxidized to either 4-aminophenol or nitrobenzene and finally is mineralized to CO_2 and H_2O generally through a quinone pathway [21]. In a system of persulfate catalyzed by magnetic $BiFeO_3$ nanoparticles, the initiation of aniline degradation by SO_4^{-} and $OH^{\bullet}$ also formed $C_6H_5NH_2^{\bullet+}$. But more intermediates other than 4-aminophenol and nitrobenzene, such as phenol and 4,4-diaminodiphenyl, were also proposed [53]. But in the present sediment–activated persulfate system, an isomer of 4-aminophenol and a secondary amine product $C_{12}H_{10}ON_2$ were first identified. Some studies have made observations about the rapid reactivity between hydroxylamine and manganese or iron-bearing minerals associated with soils or aquifer materials [56]. However, the mechanism involved in the degradation process of aniline in the presence of the aquifer sediments and persulfate (discussed below) as illustrated by the data presented suggested that identification of phenylhydroxylamine, 4-aminophenol and other oxidation byproducts like azoxybenzene in our degradation system is reasonable [49,50]. Therefore, the aniline degradation pathways should be variable in different persulfate systems.

In our system, a notable amount of aniline was still degraded despite the high mole ratio of radical scavengers were used in the quenching experiments. A computational study has proved that aniline can be oxidized by persulfate directly (Eqs. (6) and (7)) [57]. The generation of aniline nitrenium cation is the characteristic feature of all known aniline oxidation with persulfate in an extensive pH range, but it represents a rate-determining step [57]. In diluted aqueous solutions, aniline cations can react with H_2O and form C_6H_7ON (Eq. (8)).

$$C_6H_5NH_2 + S_2O_8^{2-} \rightarrow C_6H_5NH_2^{\bullet+} + SO_4^{2-} + SO_4^{\bullet-} \qquad (6)$$

$$C_6H_5NH_2^{\bullet+} + SO_4^{\bullet+} \rightarrow C_6H_5NH^+ + SO_4^{2-} + H^+ \qquad (7)$$

$$C_6H_5NH^+ + H_2O \rightarrow C_6H_7ON + H^+ \qquad (8)$$

However, Fig. 1 shows that aniline was not oxidized by persulfate without sediment. But in the presence of the sediments, there is a strong indication that the reactions of Eqs. (6)–(8) were prevalent in our system. Interestingly, Fig. S8 illustrated that the degradation process was significantly inhibited by radical scavengers ethanol and methanol, revealing that SO_4^{-} was the dominant radical responsible for aniline degradation in the absence of the aquifer sediments. Data presented in Fig. S1 shows that persulfate consumption is significantly enhanced when aniline concentration was increased (0–1 mM) in the presence of the sediments. This implies that the aquifer sediments facilitated the degradation mechanism between aniline and persulfate [16,57].

It has been reported that SO_4^{-} is the dominant active species for the degradation of aniline in ZVI–activated persulfate system [21], persulfate catalyzed by magnetic $BiFeO_3$ nanoparticles [53] and the electro-activated persulfate oxidation [22], probably due to the high reaction rate ($7.7 \pm 0.5 \times 10^9 \ M^{-1} \ s^{-1}$) of aniline with SO_4^{-} (Eq. (1)). The rate constants of the reactions between quenchers ethanol, methanol, and TBA were 1.6–7.7×10^7, 3.2×10^6 and 4.0–$9.1 \times 10^5 \ M^{-1} \ s^{-1}$, respectively [45,46]. The decline observed in the degradation rate of aniline (Fig. 4b) as a result of the addition of these quenching agents suggests that sulphate, hydroxyl and Fe(IV) species were all involved in the degradation process [45,47], yet, the amount of aniline removed was not inhibited. Therefore, aniline is competitive to consume these reactive species, and the lack of influence of radical traps in the quenching experiments revealed the involvement of direct oxidation mechanism between aniline and persulfate as reported in previous studies [16,57] since the data indicated that this phenomenon only occurred in the presence of the aquifer sediments. Nevertheless, the mechanism for the catalyzation of sediment on the direct reaction between aniline and persulfate is unknown. Some redox-active and reversible species (e.g. metals and organic matters) in the sediment may serve as the reactive moieties for electron shuttling. However, it needs further evidence to prove this hypothesis.

The proposed pathway of aniline degradation in the sediment-activated persulfate system is summarized, as illustrated in Fig. 6. Shortly, the $\equiv$Fe(II) on the surface of sediment interacts with persulfate to produce SO_4^{-} and $OH^{\bullet}$ that oxidize aniline to form aniline nitrenium cation, and then transformed to 4-aminophenol and phenylhydroxylamine. The 4-aminophenol can be oxidized by $OH^{\bullet}$ to yield benzoquinone imine and then further to be ring cleavage. The phenylhydroxylamine is dimerized and then oxidized to azoxybenzene. The azoxybenzene is not persistent in this oxidative system and further decomposed in 24 h. The production and degradation of azoxybenzene were consistent with the appearance and disappearance of the yellow-brown color of the reaction solution. However, the pathway of azoxybenzene degradation is still mysterious and need further study.

4.3. Factors on the aniline degradation in the sediment-persulfate system

It is widely accepted that using higher persulfate concentration would form the higher level of oxidizing species and then enhance the removal efficiencies of contaminants in the groundwater environment [24,58]. However, in the systems that ZVI and $BiFeO_3$ nanoparticles as activators, the persulfate above 2.5–5.0 mM induced the decline of aniline degradation rate because persulfate acts as a SO_4^{-} scavenger and as a SO_4^{-} generator [21,53].

$$SO_4^{\bullet-} + S_2O_8^{2-} \rightarrow SO_4^{2-} + S_2O_8^{\bullet-} \qquad (9)$$

$$SO_4^{2-} + SO_4^{2-} \rightarrow S_2O_8^{2-} \qquad (10)$$

Our results show that the aniline degradation rate is positively proportional to the persulfate concentration from 0 to 50 mM. Therefore, the effect of persulfate dosage on aniline degradation depends on the activator. The relationship between sediment amount and rate constant fits an exponential model. The increase of sediment amount from 10 to 30 g showed a slight enhancement of aniline degradation (Fig. S3). Liu et al. (2014) proposed the formation of persulfate radical (Eq. (11)) by the reduction of $\equiv$Fe(III) associated with the aquifer sediment to $\equiv$Fe(II) by persulfate [26]. However, this reaction is a rate-determining step for $\equiv$Fe(II) generation and slow [26]. The contribution of this mechanism needs further study.

$$\equiv Fe(III) + S_2O_8^{2-} \rightarrow \equiv Fe(II) + S_2O_8^{\bullet-} \qquad (11)$$
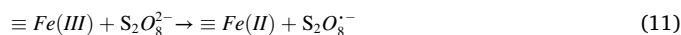
As shown in Table 1, the sediment contains 4.85 mg g^{-1} TOC. Some small organic molecules in the sediment may serve as electron shuttlings to promote the direct reaction between aniline and persulfate. Besides only a slight amount of this electron shuttlings may be enough for the activation of direct reaction. Therefore, a certain amount of sediment (10–30 g in 50 mL reaction system) is sufficient to facilitate aniline degradation. However, this hypothesis needs further evidence to be proved.

Aniline concentration is also an essential factor in its degradation rate. Hussain et al. (2014) reported that the initial amount of aniline from 0.05 to 0.40 mM negatively affected its degradation rate in ZVI activated persulfate system, and the retarding of aniline degradation was probably due to the coverage of iron surface and active sites for persulfate [21]. Our results concede with the above conclusion. The aniline degradation rate was also retarded by increasing the amount of aniline (Fig. 3c). Our discussions in the previous sections suggested that the degradation system involved both radical and direct-oxidation pathways. We agree that the increased amount of aniline will cover sediment surface and active sites of persulfate in the radical induced pathway. For the direct-oxidation pathway, it is reasonable that a lower proportion of aniline (C/C_0) was degraded at higher aniline concentrations due to the limitation of persulfate.

Traditionally, it is assumed that the components in groundwater such as HCO_3^-, Cl^-, and NOM have an overall negative impact on the activated persulfate performance due to the scavenging of free radicals [29]. A
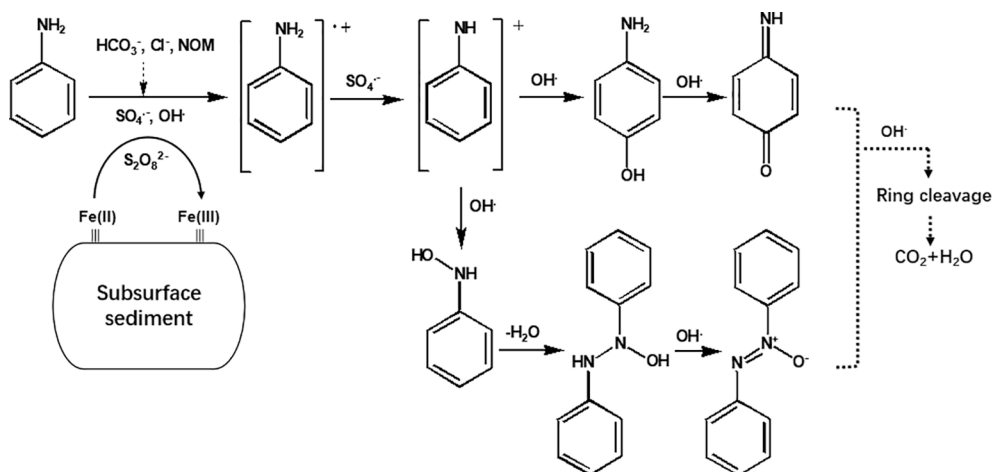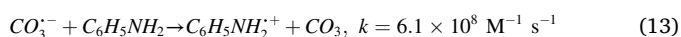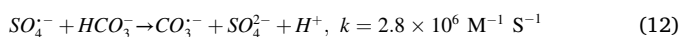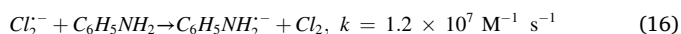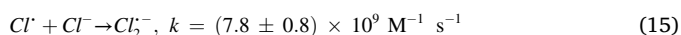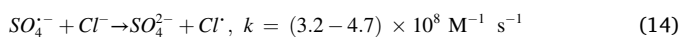
Fig. 6. The proposed mechanism of aniline degradation and mineralization in the sediment-activated persulfate system.

previous study revealed that HCO_3^- can consume $SO_4^{\cdot-}$ [29], and the formed $CO_3^{\cdot-}$ are highly reactive with aniline [29,59]. The reactions are as below.

$$SO_4^{\cdot-} + HCO_3^- \rightarrow CO_3^{\cdot-} + SO_4^{2-} + H^+, \ k = 2.8 \times 10^6 \ M^{-1} \ S^{-1} \quad (12)$$

$$CO_3^{\cdot-} + C_6H_5NH_2 \rightarrow C_6H_5NH_2^{\cdot+} + CO_3, \ k = 6.1 \times 10^8 \ M^{-1} \ s^{-1} \quad (13)$$

However, the scavenging influence of this reaction is most effective in radical based oxidation processes [16], and comparatively, the rate constant of the reaction between aniline and $SO_4^{\cdot-}$ (Eq. (1)) is much higher [28]. Therefore, the presence of HCO_3^- is supposed to inhibit the aniline degradation. However, our results indicated that low concentration of HCO_3^- (<50 mM) did not affect the degradation of aniline whereas high levels (50 and 100 mM) of HCO_3^- notably accelerated the oxidation process. We have noticed the ion H^+ is produced in both radical and direct oxidation pathways (Eqs. (4), (5), (7), (8)). The presence of HCO_3^- can react with the formed H^+ and consequently promote the above reaction. Therefore, HCO_3^- has bidirectional impacts on aniline degradation. The enhancement of aniline degradation by the higher concentrations of HCO_3^- should be due to the exceeding of the positive impact.

The chloride ion can also scavenge $SO_4^{\cdot-}$ (Eq. (14)) [60,61]. But a previous study observed that dichloride radicals ($Cl_2^{\cdot-}$) were produced (Eq. (15)) which could react with aniline to form aniline radicals (Eq. (16)) [60,62].

$$SO_4^{\cdot-} + Cl^- \rightarrow SO_4^{2-} + Cl^\cdot, \ k = (3.2 - 4.7) \times 10^8 \ M^{-1} \ s^{-1} \quad (14)$$

$$Cl^\cdot + Cl^- \rightarrow Cl_2^{\cdot-}, \ k = (7.8 \pm 0.8) \times 10^9 \ M^{-1} \ s^{-1} \quad (15)$$

$$Cl_2^{\cdot-} + C_6H_5NH_2 \rightarrow C_6H_5NH_2^{\cdot-} + Cl_2, \ k = 1.2 \times 10^7 \ M^{-1} \ s^{-1} \quad (16)$$

However, the reaction rates of Eqs. (14) and (16) are much lower than Eq. (1). As a result, the contribution of this reaction towards aniline degradation is negligible in our oxidation system.

Natural organic matter is regarded as a complex mixture of aliphatic and aromatic components that acts as a sink and scavenges for reactive oxygen species like $SO_4^{\cdot-}$ and $OH^\cdot$ [30,31]. Based on the carbon in NOM in their research, the reaction rate of $SO_4^{\cdot-}$ with NOM is $(0.6–1.2) \times 10^6$ $M^{-1} s^{-1}$ (Eq. (18)) which is much lower than that of Eq. (1). However, as shown in Eq. (6), data from quenching experiments indicated that aniline could be degraded by a non-radical pathway in the presence of the aquifer sediments and persulfate. Consequently, the addition of HA showed no impact on aniline degradation in our system.

$$SO_4^{\cdot-} + NOM \rightarrow products, \ k = (0.6 - 1.2) \times 10^6 \ M^{-1} \ s^{-1} \quad (18)$$
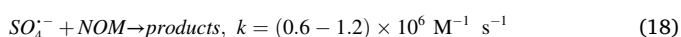
In summary, the negligible impacts of HCO_3^- (low level), Cl^-, and

NOM on aniline degradation are not only due to the competitive reaction between aniline and $SO_4^{\cdot-}$ but also as a result of the direct oxidation reaction between persulfate and aniline.

5. Conclusion

Findings from our investigation demonstrated that the subsurface sediment could activate persulfate for aniline degradation. More than 90% aniline was removed in 6 h when the persulfate concentrations ranged from 10 to 50 mM, the sediment amounts varied from 10 to 30 g, and the aniline concentrations were tested from 0.05 to 1.0 mM in 50 mL reaction system. The levels of persulfate, sediment, and aniline impact the degradation rate of aniline and stoichiometric efficiency of the treatment system. The groundwater components such as Cl^- (0–100 mM), HA (0–5 mg C L^{-1}), and HCO_3^- (0–20 mM) induced no significant deviation of aniline degradation rates but rather enhanced persulfate consumption. However, higher concentrations of HCO_3^- (50 and 100 mM) caused faster aniline degradation. These results demonstrate that persulfate can be used for *in-situ* remediation of aniline contaminated groundwater activated by the subsurface sediment.

Our findings also provide the mechanism of aniline degradation by sediment–activated persulfate. The $\equiv$Fe(II) especially Fe(II)-O complex in the sediment can interact with persulfate to produce $SO_4^{\cdot-}$, $OH^\cdot$ and Fe(IV). Besides, the results further suggest that the presence of the sediments simultaneously facilitated a non-radical mechanism that oxidizes aniline. In this system, aniline was degraded to form such intermediates as 4-aminophenol, phenylhydroxylamine, and azoxybenzene, which can be further degraded and mineralized. The formation of azoxybenzene should be noticed as its degradation pathway is still unknown in our system. Therefore, our observations urge the re-evaluation when employing *in-situ* subsurface sediment as an activator for remediation purposes since each contaminant may demonstrate a different degradation mechanism.

Declaration of Competing Interest

The authors declare that they have no known competing financial interests or personal relationships that could have appeared to influence the work reported in this paper.

Acknowledgements

Appendix A. Supplementary data

Figs. S1–S8. And the data including HPLC-MS data for 5 samples, XPS data for 2 samples, and the data for Figs. 1, 2, 4 have been deposited to the repository as Mendeley data. Supplementary data to this article can be found online at https://doi.org/10.1016/j.cej.2020.128078.

References

[1] Y. Zhou, Y.X. Wang, Y.Y. Li, F. Zwahlen, J. Boillat, Hydrogeochemical characteristics of central Jianghan Plain, China, Environ. Earth. Sci. 68 (2012) 765–778.

[2] M.F. Khan, X. Wu, B.S. Kaphalia, P.J. Boor, G.A. Ansari, Nitrotyrosine formation in splenic toxicity of aniline, Toxicology 194 (2003) 95–102.

[3] B. Kang, D. Wang, S.H. Du, Source identification and degradation pathway of multiple persistent organic pollutants in groundwater at an abandoned chemical site in Hebei, China, Exp. Health 9 (2016) 135–141.

[4] D.S. Kosson, S.V. Byrne, Interactions of aniline with soil and groundwater at an industrial spill site, Environ. Health Perspect. 103 (Suppl. 5) (1995) 71–73.

[5] R.J. Portier, G.P. Curole, R.M. Conger, L.M. Basirico, C. Metosh-Dickey, In situ bioremediation of an aniline spill in an industrial setting, Remediation 20 (2010) 105–117.

[6] Y.J. Wen, Y.S. Yang, H.J. Ren, X.Q. Du, X.Y. Yang, L.Y. Zhang, X.S. Wang, Chemical–biological hybrid reactive zones and their impact on biodiversity of remediation of the nitrobenzene and aniline contaminated groundwater, Chem. Eng. J. 280 (2015) 233–240.

[7] M.N. Huda Bhuiyan, H. Kang, J.H. Kim, S. Kim, Y. Kho, K. Choi, Endocrine disruption by several aniline derivatives and related mechanisms in a human adrenal H295R cell line and adult male zebrafish, Ecotoxicol. Environ. Saf. 180 (2019) 326–332.

[8] A. Tsitonaki, B. Petri, M. Crimi, H. Mosbaek, R.L. Siegrist, P.L. Bjerg, In situ chemical oxidation of contaminated soil and groundwater using persulfate: a review, Crit. Rev. Environ. Sci. Technol. 40 (2010) 55–91.

[9] D. Zingaretti, I. Verginelli, R. Baciocchi, Catalyzed hydrogen peroxide combined with CO_2 sparging for the treatment of contaminated groundwater, Chem. Eng. J. 300 (2016) 119–126.

[10] J. Cui, L. Zhang, B. Xi, J. Zhang, X. Mao, Chemical oxidation of benzene and trichloroethylene by a combination of peroxymonosulfate and permanganate linked by in-situ generated colloidal/amorphous MnO_2, Chem. Eng. J. 313 (2017) 815–825.

[11] Y. Vera, R. de Carvalho, M. Torem, B. Calfa, Atrazine degradation by in situ electrochemically generated ozone, Chem. Eng. J. 155 (2009) 691–697.

[12] H. Dong, K. Hou, W. Qiao, Y. Cheng, L. Zhang, B. Wang, L. Li, Y. Wang, Q. Ning, G. Zeng, Insights into enhanced removal of TCE utilizing sulfide-modified nanoscale zero-valent iron activated persulfate, Chem. Eng. J. 359 (2019) 1046–1055.

[13] F. Jiang, Y. Li, W. Zhou, Z. Yang, Y. Ning, D. Liu, Z. Tang, S. Yang, H. Huang, G. Wang, Enhanced degradation of monochlorobenzene in groundwater by ferrous iron/persulfate process with cysteine, Chem. Eng. J. 387 (2020) 124048.

[14] X. Li, B. Wu, Q. Zhang, D. Xu, Y. Liu, F. Ma, Q. Gu, F. Li, Mechanisms on the impacts of humic acids on persulfate/Fe^{2+}-based groundwater remediation, Chem. Eng. J. 378 (2019), 122142.

[15] L.W. Matzek, K.E. Carter, Activated persulfate for organic chemical degradation: a review, Chemosphere 151 (2016) 178–188.

[16] S. Wacławek, H.V. Lutze, K. Grübel, V.V.T. Padil, M. Černík, D.D. Dionysiou, Chemistry of persulfates in water and wastewater treatment: a review, Chem. Eng. J. 330 (2017) 44–62.

[17] N. Zrinyi, A.L.T. Pham, Oxidation of benzoic acid by heat-activated persulfate: effect of temperature on transformation pathway and product distribution, Water Res. 120 (2017) 43–51.

[18] Y.C. Zhang, Q. Zhang, Z.Y. Dong, L.Y. Wu, J.M. Hong, Degradation of acetaminophen with ferrous/copperoxide activate persulfate: synergism of iron and copper, Water Res. 146 (2018) 232–243.

[19] X.X. Pan, J. Chen, N.N. Wu, Y.M. Qi, X.X. Xu, J.L. Ge, X.H. Wang, C.G. Li, R.J. Qu, V.K. Sharma, Z.Y. Wang, Degradation of aqueous 2,4,4′-trihydroxybenzophenone by persulfate activated with nitrogen doped carbonaceous materials and the formation of dimer products, Water Res. 143 (2018) 176–187.

[20] Y. Wu, J. Guo, Y. Han, J. Zhu, L. Zhou, Y. Lan, Insights into the mechanism of persulfate activated by rice straw biochar for the degradation of aniline, Chemosphere 200 (2018) 373–379.

[21] I. Hussain, Y.Q. Zhang, S.B. Huang, Degradation of aniline with zero-valent iron as an activator of persulfate in aqueous solution, RSC Adv. 4 (2014) 3502–3511.

[22] W.S. Chen, C.P. Huang, Mineralization of aniline in aqueous solution by electrochemical activation of persulfate, Chemosphere 125 (2015) 175–181.

[23] W.-S. Chen, C.-P. Huang, Mineralization of aniline in aqueous solution by electro-activated persulfate oxidation enhanced with ultrasound, Chem. Eng. J. 266 (2015) 279–288.

[24] X. Xie, Y. Zhang, W. Huang, S. Huang, Degradation kinetics and mechanism of aniline by heat-assisted persulfate oxidation, J. Environ. Sci. (China) 24 (2012) 821–826.

[25] K.S. Sra, N.R. Thomson, J.F. Barker, Persistence of persulfate in uncontaminated aquifer materials, Environ. Sci. Technol. 44 (2010) 3098–3104.

[26] H. Liu, T.A. Bruton, F.M. Doyle, D.L. Sedlak, In situ chemical oxidation of contaminated groundwater by persulfate: decomposition by Fe(III)- and Mn(IV)-containing oxides and aquifer materials, Environ. Sci. Technol. 48 (2014) 10330–10336.

[27] N. Yan, H. Zhong, M.L. Brusseau, The natural activation ability of subsurface media to promote in-situ chemical oxidation of 1,4-dioxane, Water Res. 149 (2019) 386–393.

[28] Y.N. Yuan, T. Luo, J. Xu, J.J. Li, F. Wu, M. Brigante, G. Mailhot, Enhanced oxidation of aniline using Fe(III)-S(IV) system: role of different oxysulfur radicals, Chem. Eng. J. 362 (2019) 183–189.

[29] L.R. Bennedsen, J. Muff, E.G. Sogaard, Influence of chloride and carbonates on the reactivity of activated persulfate, Chemosphere 86 (2012) 1092–1097.

[30] Z.Y. Wang, Y.S. Shao, N.Y. Gao, X. Lu, N. An, Degradation kinetic of phthalate esters and the formation of brominated byproducts in heat-activated persulfate system, Chem. Eng. J. 359 (2019) 1086–1096.

[31] L. Zhou, M. Sleiman, C. Ferronato, J.M. Chovelon, C. Richard, Reactivity of sulfate radicals with natural organic matters, Environ. Chem. Lett. 15 (2017) 733–737.

[32] J. Ma, H. Liu, L. Tong, Y. Wang, S. Liu, L. Zhao, L. Hou, Source apportionment of polycyclic aromatic hydrocarbons and n-alkanes in the soil-sediment profile of Jianghan Oil Field, China, Environ. Sci. Pollut. Res. Int. 24 (2017) 13344–13351.

[33] M. Tong, S. Yuan, S. Ma, M. Jin, D. Liu, D. Cheng, X. Liu, Y. Gan, Y. Wang, Production of abundant hydroxyl radicals from oxygenation of subsurface sediments, Environ. Sci. Technol. 50 (2016) 214–221.

[34] G. Fang, J. Gao, D.D. Dionysiou, C. Liu, D. Zhou, Activation of persulfate by quinones: free radical reactions and implication for the degradation of PCBs, Environ. Sci. Technol. 47 (2013) 4605–4611.

[35] Y. Wang, H. Liu, Y.E. Peng, L. Tong, L. Feng, K.S. Ma, New pathways for the biodegradation of diethyl phthalate by *Sphingobium yanoikuyae* SHJ, Process Biochem. 71 (2018) 152–158.

[36] C. Liang, C.F. Huang, N. Mohanty, R.M. Kurakalva, A rapid spectrophotometric determination of persulfate anion in ISCO, Chemosphere 73 (2008) 1540–1543.

[37] Y.T. Zhang, M. Tong, S.H. Yuan, A. Qian, H. Liu, Interplay between iron species transformation and hydroxyl radicals production in soils and sediments during anoxic-oxic cycles, Geoderma 370 (2020), 114351.

[38] H. Liu, T.A. Bruton, W. Li, J.V. Buren, C. Prasse, F.M. Doyle, D.L. Sedlak, Oxidation of benzene by persulfate in the presence of Fe(III)- and Mn(IV)-containing oxides: stoichiometric efficiency and transformation products, Environ. Sci. Technol. 50 (2016) 890–898.

[39] A.L. Pham, F.M. Doyle, D.L. Sedlak, Kinetics and efficiency of H_2O_2 activation by iron-containing minerals and aquifer materials, Water Res. 46 (2012) 6454–6462.

[40] B.J. Ouyang, X.C. Lu, H. Liu, J. Li, T.T. Zhu, X.Y. Zhu, J.J. Lu, R.C. Wang, Reduction of jarosite by *Shewanella oneidensis* MR-1 and secondary mineralization, Geochim. Cosmochim. Acta 124 (2014) 54–71.

[41] M. Descostes, F. Mercier, N. Thromat, C. Beaucaire, M. Gautier-Soyer, Use of XPS in the determination of chemical environment and oxidation state of iron and sulfur samples: constitution of a data basis in binding energies for Fe and S reference compounds and applications to the evidence of surface species of an oxidized pyrite in a carbonate medium, Appl. Surf. Sci. 165 (2000) 288–302.

[42] X.H. Zhang, Y.Z. Chen, N. Zhao, H. Liu, Y. Wei, Citrate modified ferrihydrite microstructures: facile synthesis, strong adsorption and excellent Fenton-like catalytic properties, RSC Adv. 4 (2014) 21575–21583.

[43] R.S. Cutting, V.S. Coker, J.W. Fellowes, J.R. Lloyd, D.J. Vaughan, Mineralogical and morphological constraints on the reduction of Fe(III) minerals by Geobacter sulfurreducens, Geochim. Cosmochim. Acta 73 (2009) 4004–4022.

[44] A.R. Pratt, Vivianite auto-oxidation, Phys. Chem. Miner. 25 (1997) 24–27.

[45] G.P. Anipsitakis, D.D. Dionysiou, Radical generation by the interaction of transition metals with common oxidants, Environ. Sci. Technol. 38 (2004) 3705–3712.

[46] G.V. Buxton, C.L. Greenstock, W.P. Helman, A.B. Ross, Critical review of rate constants for reactions of hydrated electrons, hydrogen atoms and hydroxyl radicals (OH/O) in aqueous solution, J. Phys. Chem. Ref. Data 17 (1988) 513.

[47] Z. Wang, W. Qiu, S.Y. Pang, Y. Zhou, Y. Gan, C.T. Guan, J. Jiang, Further understanding the involvement of Fe(IV) in peroxydisulfate and peroxymonosulfate activation by Fe(II) for oxidative water treatment, Chem. Eng. J. 371 (2019) 842–847.

[48] Z. Wang, W. Qiu, S. Pang, Y. Gao, Y. Zhou, Y. Cao, J. Jiang, Relative contribution of ferryl ion species (Fe(IV)) and sulfate radical formed in nanoscale zero valent iron activated peroxydisulfate and peroxymonosulfate processes, Water Res. 172 (2020), 115504.

[49] E.J. Behrman, Studies on the reaction between peroxydisulfate ions and aromatic amines. Boyland-Sims oxidation, J. Am. Chem. Soc. 89 (1967) 2424–2428.

[50] E.J. Behrman, The Ortho-Para Ratio and the Intermediate in the Persulfate oxidation of aromatic-amines (the Boyland-Sims oxidation), Am. J. Org. Chem. 57 (1992) 2266–2270.

[51] T. Olmez-Hanci, I. Arslan-Alaton, B. Genc, Bisphenol A treatment by the hot persulfate process: oxidation products and acute toxicity, J. Hazard. Mater. 263 (Pt 2) (2013) 283–290.

[52] Y.Q. Gao, N.Y. Gao, D.Q. Yin, F.X. Tian, Q.F. Zheng, Oxidation of the beta-blocker propranolol by UV/persulfate: effect, mechanism and toxicity investigation, Chemosphere 201 (2018) 50–58.

[53] I. Hussain, Y.Q. Zhang, M.Y. Li, S.B. Huang, W. Hayat, L.M. He, X.D. Du, G.Q. Liu, M.M. Du, Heterogeneously degradation of aniline in aqueous solution using persulfate catalyzed by magnetic $BiFeO_3$ nanoparticles, Catal. Today 310 (2018) 130–140.

[54] B.G. Petri, R.J. Watts, A. Tsitonaki, M. Crimi, N.R. Thomson, A.L. Teel, Fundamentals of ISCO using persulfate, in: R.L. Siegrist, M. Crimi, T.J. Simpkin (Eds.), In Situ Chemical Oxidation for Groundwater Remediation, Springer, New York, New York, NY, 2011, pp. 147–191.

[55] H.Y. Dong, Y. Li, S.C. Wang, W.F. Liu, G.M. Zhou, Y.F. Xie, X.H. Guan, Both Fe(IV) and radicals are active oxidants in the Fe(II)/peroxydisulfate process, Environ. Sci. Technol. Lett. 7 (2020) 219–224.

[56] K. Rue, K. Rusevova, C.L. Biles, S.G. Huling, Abiotic hydroxylamine nitrification involving manganese- and iron-bearing minerals, Sci. Total Environ. 644 (2018) 567–575.

[57] B. Marjanovic, I. Juranic, G. Ciric-Marjanovic, Revised mechanism of Boyland-Sims oxidation, J. Phys. Chem. A 115 (2011) 3536–3550.

[58] Y. Zhou, Y. Xiang, Y. He, Y. Yang, J. Zhang, L. Luo, H. Peng, C. Dai, F. Zhu, L. Tang, Applications and factors influencing of the persulfate-based advanced oxidation processes for the remediation of groundwater and soil contaminated with organic compounds, J. Hazard. Mater. 359 (2018) 396–407.

[59] S. Canonica, T. Kohn, M. Mac, F.J. Real, J. Wirz, U. von Gunten, Photosensitizer method to determine rate constants for the reaction of carbonate radical with organic compounds, Environ. Sci. Technol. 39 (2005) 9182–9188.

[60] X.Y. Yu, Z.Y. Bao, J.R. Barker, Free radical reactions involving Cl, Cl_2, and SO_4 in the 248 nm photolysis of aqueous solutions containing $S_2O_8^{2}$ and Cl, J. Phys. Chem. A 108 (2004) 295–308.

[61] M.C. Lu, Y.F. Chang, I.M. Chen, Y.Y. Huang, Effect of chloride ions on the oxidation of aniline by Fenton's reagent, J. Environ. Manage. 75 (2005) 177–182.

[62] K. Hasegawa, P. Neta, Rate constant and mechanisms of reaction of Cl_2 radicals, J. Phys. Chem. 82 (1978) 854–857.